DOI: 10.1002/ejic.201000835

An Imidazolate- and Azide-Bridged Copper(II) Coordination Polymer Consisting of Alternating Di- and Mononuclear Units

Ken-ichi Sakai,*[a] Tomoyuki Akutagawa,[b] and Takayoshi Nakamura[c]

Keywords: Coordination polymers / Copper / N ligands / Azides / Magnetic properties

Using the Cu^{II}-imidazole(Him) complex $[Cu(Him)_4Cl]Cl$ as the starting material, the imidazolate (im)- and azide-bridged Cu^{II} coordination polymer $[Cu_3(Him)_4(im)_2(N_3)_4]_n$ was successfully obtained. Single-crystal X-ray analysis revealed that it possesses an im-bridged linear-chain structure consisting of alternating dinuclear units with a symmetric end-on azide-bridged $[Cu(\mu_{1,1}\text{-}N_3)_2Cu]^{2+}$ core and mononuclear units. All of the Cu ions adopt a square pyramidal geometry with an azide at the Jahn–Teller elongated apical position. Some of the azides act as end-to-end interchain bridging ligands from the mononuclear unit to the nearest neighbouring dinuclear unit of the adjacent chain forming a two-dimensional network. Temperature-variable magnetic susceptibility measurements showed that it exhibits one-dimensional ferrimagnetic-like behaviour, which can be ascribed to two types of exchange couplings with opposite signs, namely a weak ferromagnetic coupling through the end-on azide bridges within the dinuclear units and a stronger antiferromagnetic coupling through the im bridges between the di- and the mononuclear units.

Introduction

Recently, coordination polymers have received much attention owing to their potential use in various applications.[1–6] Bridging ligands linking adjacent metal ions are of two types, namely inorganic and organic, and their choice, design and combination are particularly important for imparting functionalities to the system. Azide is one of the most widely used inorganic bridging ligands and is especially effective in the construction of molecule-based magnets.[7–10] In many of the azide-bridged coordination polymers reported so far, the unique topological and magnetic properties are mainly achieved through the two typical coordination modes of the azide, namely the end-on (EO) ($\mu_{1,1}$-N_3) and the end-to-end (EE) ($\mu_{1,3}$-N_3) modes, which provide ferromagnetic and antiferromagnetic interactions between spins on the neighbouring metal ions, respectively. On the other hand, among the organic bridging ligands, the simplest and most compact heterocycle is an imidazolate (im), which is a deprotonated form of imidazole (Him). Him is a functional group of histidine and plays a biologically significant role as a metal ligand in constructing an active centre in metalloproteins, such as superoxide dismutase, which has an im-bridged dinuclear metal centre. Thus, numerous metal complexes with Him/im ligands have been prepared and investigated.[11–18] Furthermore, recent interest has been directed towards the im-based materials called zeolitic im frameworks (ZIFs) because of their catalytic applications.[19] However, Him/im-based coordination polymers are not very numerous,[20–26] probably due to the lack of structural information resulting from the difficulty of growing single-crystals. In practice, recent successful syntheses have been achieved by using superior methods such as the hydrothermal synthesis,[22,23] the solvolysis of carbonyldiimidazole[24,25] and synthesis using ionic liquid.[26] Structurally simple ligands such as azide and Him/im are expected to provide novel coordination polymers with both topological and magnetic diversity.[27,28] However, growing single-crystals of the products is going to be difficult if the ligands are directly mixed with metal ions under the usual conditions. Thus, we focused on using the five-coordinate Cu^{II}-Him complex of $[Cu(Him)_4Cl]Cl$ as a starting building block.[18] As a result of an attempt to exchange the chloride ions for azides, single-crystals of a novel Cu^{II} coordination polymer $[Cu_3(Him)_4(im)_2(N_3)_4]_n$ were successfully obtained by simply mixing the complex and sodium azide together in solution. Herein we report the crystal structure and magnetic properties of the novel complex.

[a] Department of Bio- & Material Photonics, Chitose Institute of Science and Technology (CIST),
Bibi, Chitose 066-8655, Japan
Fax: +81-123-27-6054
E-mail: k-sakai@photon.chitose.ac.jp
[b] Polymer Hybrid Materials Research Center, Institute of Multidisciplinary Research for Advanced Materials (IMRAS), Tohoku University, Sendai 980-8577, Japan
[c] Research Institute for Electronic Science (RIES), Hokkaido University,
Sapporo 001-0020, Japan

Results and Discussion

Crystal Structure

The crystal structure of $[Cu_3(Him)_4(im)_2(N_3)_4]_n$ is shown in Figure 1. It has im-bridged linear chain structures con-

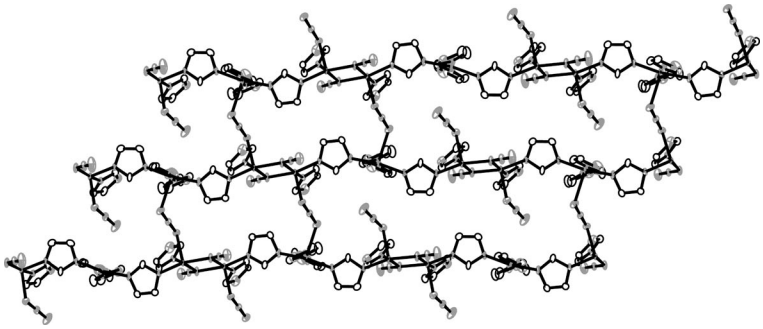

Figure 1. The crystal structure of $[Cu_3(Him)_4(im)_2(N_3)_4]_n$. The hydrogen atoms are omitted for clarity.

sisting of alternating di- and mononuclear Cu^{II} units, which are partly linked to each other by EE azide bridges forming a two-dimensional network. The schematic diagram of the complex is depicted in Scheme 1. There are two types of dinuclear units, namely $[Cu_2(Him)_2(im)_2(\mu_{1,1}\text{-}N_3)_2(\mu_{1,3}\text{-}N_3)_2]^{2-}$ and $[Cu_2(Him)_2(im)_2(\mu_{1,1}\text{-}N_3)_2(N_3)_2]^{2-}$ denoted by D and D′, respectively. In both units, the first azides $(\mu_{1,1}\text{-}N_3)_2$ are EO bridges that construct a dinuclear core $[Cu(\mu_{1,1}\text{-}N_3)_2Cu]^{2+}$. However, the other azides in D act as EE bridges linking the adjacent chains together, while those in D′ are non-bridging ligands. All the mononuclear units are described as $[Cu(Him)_2(im)_2(\mu_{1,3}\text{-}N_3)]^-$ (denoted by M), where the azide is one of the two EE bridges in D. Overall the -D-M-D′-M- pattern is repeated in the chain direction and the M-D-M set cross-links three chains in the interchain direction.

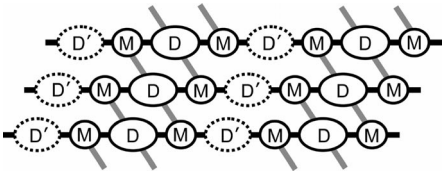

Scheme 1. A schematic diagram of the packing arrangements in the $[Cu_3(Him)_4(im)_2(N_3)_4]_n$ crystal. D,D′ and M represent $[Cu_2(Him)_2(im)_2(\mu_{1,1}\text{-}N_3)_2(\mu_{1,3}\text{-}N_3)_2]^{2-}$, $[Cu_2(Him)_2(im)_2(\mu_{1,1}\text{-}N_3)_2(N_3)_2]^{2-}$ and $[Cu(Him)_2(im)_2(\mu_{1,3}\text{-}N_3)]^-$, respectively. An im bridge is found between the M and D or D′ units in the chain direction, while an EE azide is found between the D and M units in the interchain direction.

The ORTEP drawings of the interchain M-D-M and the intrachain D′-M structures are shown in Figure 2, and selected bond lengths and bond angles are listed in Table 1. To date, the double EO-azide-bridged dinuclear core $[Cu(\mu_{1,1}\text{-}N_3)_2Cu]^{2+}$ has been studied from the magneto-structural correlation perspective.[29–39] The dinuclear core of the D unit is centrosymmetric (Figure 2, a). Each Cu ion in the D unit adopts a square pyramidal geometry with the basal plane formed by four nitrogen atoms from two EO-azides, one Him and one im, and with the apical site occupied by a nitrogen atom from an EE-azide. The apical Cu3–N19 bond is elongated [2.300(5) Å] compared to the basal Cu–N bonds [1.979(4)–2.035(4) Å] due to the Jahn–Teller effect. The four N(basal)–Cu3–N19 angles fall in the narrow range of 94.4(2) to 96.6(2)°, and the two *trans* angles of the basal plane are almost equal with N11–Cu3–N22 and N10–Cu3–N22B angles of 165.6(2)° and 165.1(12)°, respectively. Thus, an ideal square pyramidal geometry is formed around the Cu ion. In fact, the distortion parameter (τ), defined on the basis of the *trans* angles of the basal plane where $\tau = 0$ for an ideal square pyramid and $\tau = 1$ for a trigonal bipyramid,[40] is calculated to be 0.01. For the dinuclear core, the Cu3–N22 and Cu3–N22B bond lengths are 2.028(3) and 2.035(4) Å, respectively, which indicates that the double EO-azide bridges of the D unit are close to symmetric. The Cu3–N–Cu3B angles are 103.6(2)°, which is located close to the critical angle between the ferromagnetic and the antiferromagnetic regimes ($\theta = 104°$).[29] The direct Cu3–Cu3B distance in D is 3.1919(8) Å.

These structural properties of D hold mostly true for D′ as well, except that the square pyramidal geometry around the copper ion has a non-bridging azide at the apical site (Figure 2, b). Although the τ value for the D′ unit is slightly increased to 0.07, the structural parameters for the dinuclear core, such as the Cu–N(azide) bond lengths and the Cu–N–Cu angles, are the same as those for D thus forming a similar symmetric core. The only remarkable difference that is observed for the mean out-of-plane deviation of the azide groups, which is 20.69° and 14.58° for D and D′, respectively.

The coordination geometry around the Cu ion in the M unit is also square pyramidal, where the basal plane is formed by the four nitrogen atoms from two Him and two im, and where the apical site is occupied by a nitrogen atom from an EE-azide (Figure 2, b). The average bond length of the two Cu–N(im) bonds (Cu2–N4 and Cu2–N9) is 2.00 Å, which is slightly shorter than the 2.02 Å of the two Cu–N(Him) bonds (Cu2–N5 and Cu2–N7). The *trans* angles of N4–Cu2–N9 and N5–Cu2–N7 are 170.2(2)° and 178.0(2)°, respectively, thereby giving $\tau = 0.13$. The apical Cu2–N21 bond is more elongated than the corresponding Cu3–N19 bond in the D unit by 0.21 Å, which suggests a stronger Jahn–Teller effect in the D′ unit. The Cu1–Cu2 and Cu2–Cu3 distances along the im-bridging direction are 5.928(1) and 6.0146(9) Å, respectively, while the Cu2–Cu3 distance along the interchain EE-azide bridging direction is 6.124(1) Å.

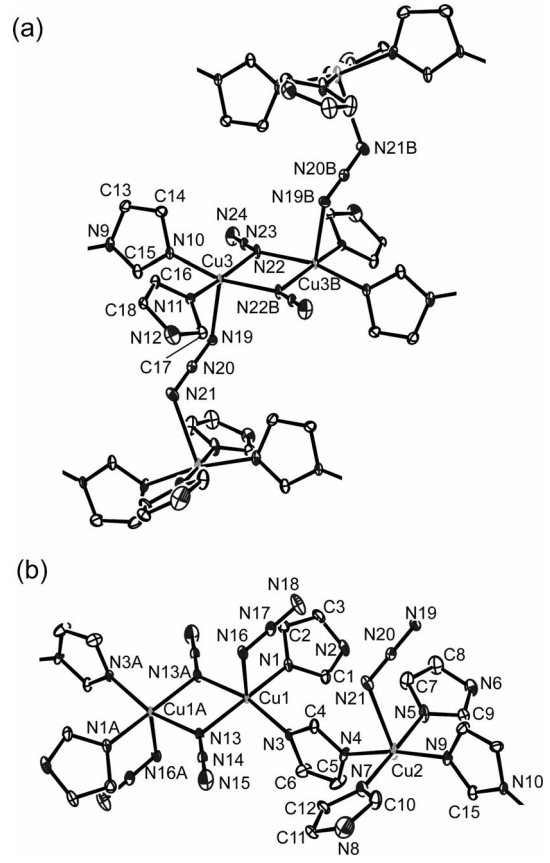

Figure 2. The ORTEP drawings (30% ellipsoid probability) of (a) the interchain M-D-M structure and (b) the intrachain D′-M structure, with atomic numbering. The hydrogen atoms are omitted for clarity. Symmetry codes A: $-x + 2, -y + 2, -z$; B: $-x + 1, -y, -z + 1$.

Table 1. Selected bond lengths [Å] and bond angles [°].[a]

Cu1–N1	1.989(3)	Cu1–N3	1.973(4)
Cu1–N13	2.013(3)	Cu1–N13A	2.031(4)
Cu2–N4	1.994(4)	Cu2–N5	2.019(4)
Cu2–N7	2.022(4)	Cu2–N9	1.998(4)
Cu3–N10	1.979(4)	Cu3–N11	1.985(3)
Cu3–N19	2.301(4)	Cu3–N22	2.028(3)
Cu3–N22B	2.035(4)		
N1–Cu1–N3	92.89(18)	N1–Cu1–N13	167.52(17)
N1–Cu1–N13A	95.86(17)	N3–Cu1–N13	92.55(17)
N3–Cu1–N13A	163.59(17)	N13–Cu1–N13A	76.30(16)
N4–Cu2–N5	89.92(18)	N4–Cu2–N7	90.29(18)
N4–Cu2–N9	170.2(2)	N5–Cu2–N7	178.0(2)
N5–Cu2–N9	91.40(18)	N7–Cu2–N9	88.72(18)
N10–Cu3–N11	93.81(17)	N10–Cu3–N19	94.45(17)
N10–Cu3–N22	92.46(16)	N10–Cu3–N22B	165.09(16)
N11–Cu3–N19	96.27(16)	N11–Cu3–N22	165.57(17)
N11–Cu3–N22B	94.91(16)	N19–Cu3–N22	96.18(17)
N19–Cu3–N22B	96.59(18)	N22–Cu3–N22B	76.44(16)

[a] Symmetry codes A: $-x + 2, -y + 2, -z$; B: $-x + 1, -y, -z + 1$.

Magnetic Properties

The magnetic susceptibility of $[Cu_3(Him)_4(im)_2(N_3)_4]_n$ was measured over a temperature range of 2 to 300 K. The χT versus T plot is shown in Figure 3. χT is 1.07 emu K/mol at 300 K, which is somewhat smaller than that expected for three magnetically isolated Cu^{II} ions (1.14 emu K/mol, which is three times 0.38 emu K/mol for an $S = 1/2$ spin with $g = 2.0$). χT decreased as the temperature decreased, reaching a minimum of 0.43 emu K/mol at 24 K and then increased to 0.57 emu K/mol at 3 K. Such magnetic behaviour is reminiscent of ferrimagnetic interactions, as observed in certain metal-azide coordination polymers.[41–44] These systems are also homometallic, which is rare. In addition, χT slightly decreased once again at 2 K to 0.54 emu K/mol (Figure 3, inset).

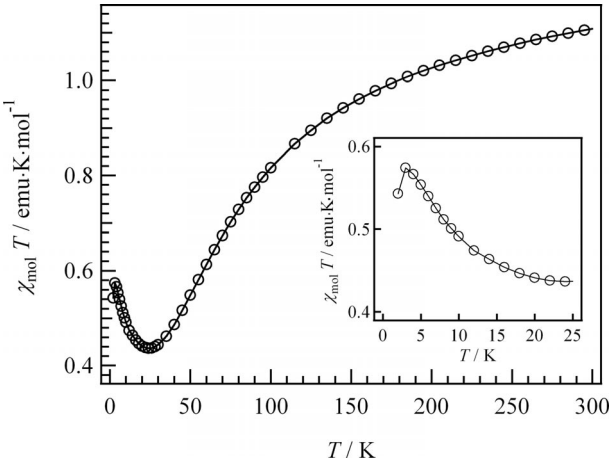

Figure 3. The χT vs. T plot for $[Cu_3(Him)_4(im)_2(N_3)_4]_n$. The inset shows the extended χT vs. T plot below 25 K.

In the present system, as shown in Scheme 2, five types of exchange couplings (J_1, J_2, J_1', J_2' and J_3) can be assumed among Cu^{II} $S = 1/2$ spins. Since it is impossible to construct a model that determines these values analytically, we considered the origin of the magnetic behaviour based on the X-ray structural data and the previously reported J values for im and azide bridges. Firstly, considering that all the Cu ions adopt a square pyramidal shape with an azide at the Jahn–Teller elongated apical position, the magnetic orbitals are the $3d_{x^2-y^2}$ orbital spread over the basal plane and not in the apical direction. Therefore, the exchange interactions through the interchain EE-azide bridge (J_3) should be low. Secondly, in the double EO-azide-bridged dinuclear core, the magnetic $3d_{x^2-y^2}$ orbitals of the basal planes are conversely responsible for causing spin coupling. For the symmetric EO-azide coordination modes, as seen in both the D and the D′ units, the exchange interactions are usually ferromagnetic. The reported J values are in the range of 23 to 230 cm^{-1}[32,33] and are known to be correlated to the Cu–N_{azide}–Cu angle (θ). As θ increases from about 85 to 104°, J gradually decreases, and finally enters the antiferromagnetic regime ($J < 0$) when $\theta \geq 104°$. Since the θ values in the D and the D′ units are 103.6(2)° and 103.7(2)°, respectively, the J values are predicted to be small even if the spins interact ferromagnetically. In addition, as long as only the θ values are considered, the assumption that $J_1 \approx J_1'$ is reasonable. Thirdly, the exchange interactions through the im bridges are usually antiferromagnetic with J values of –88 to 0 cm^{-1}.[24,45] The important struc-

tural parameter affecting J is the Cu–N_{im}···N_{im} angle (ϕ), where when ϕ is 180°, J is at the maximum value. In the im bridge between the D and the M units, the average ϕ value for Cu1–N3–N4 and Cu2–N4–N3 is 161.8°, while the corresponding value for the im bridge between the D′ and the M units is 159.0°. In a recent study with approximately the same ϕ angle (ϕ = 163.8°), a J value of –34 cm^{-1} was reported.[24] Thus, it was estimated that J_2 and J_2' are moderate and it was assumed that $J_2 \approx J_2'$.

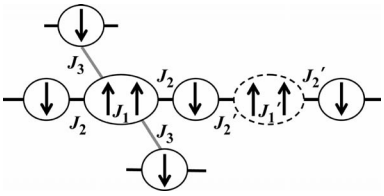

Scheme 2. A schematic diagram of the exchange coupling pathways in the $[Cu_3(Him)_4(im)_2(N_3)_4]_n$ crystal.

From the above considerations, the present system could be simplified to two types of exchange interactions with opposite signs ($J_1 > 0$, $J_2 < 0$ and $J_1 < |J_2|$) that are alternately arranged along the one-dimensional direction. Under this assumed situation, the magnetic behaviour shown in Figure 3 can be explained as follows: as the temperature decreases from 300 to 24 K, the paramagnetic population is depopulated as a reflection of the antiferromagnetic interaction through the im bridges ($J_2 < 0$), which eventually results in a decrease in the χT value. Below 24 K, the χT value increases because of the contribution of the ferromagnetic interactions within the dinucluear core ($J_1 > 0$). Such an explanation supports the observation that the present system behaves ferrimagnetically, although it is homometallic. The magnetization measurement at 2 K gave a saturation value of 0.84 $N\beta$ (Figure 4), which is approximately consistent with one spin in the monomer unit, $[Cu_3(Him)_4(im)_2(N_3)_4]$. As an additional note, the slight decrease in the χT value at 2 K may be due to the interchain antiferromagnetic coupling J_3.

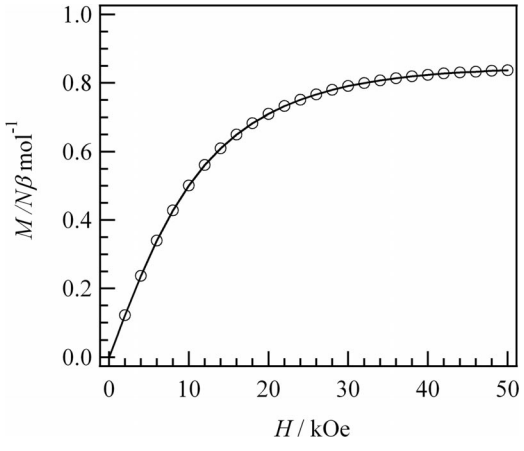

Figure 4. The field dependence of the magnetization for $[Cu_3(Him)_4(im)_2(N_3)_4]_n$ at 2 K.

Conclusions

The im- and azide-bridged Cu^{II} coordination polymer $[Cu_3(Him)_4(im)_2(N_3)_4]_n$ was prepared, and the crystal structure and magnetic properties were investigated. For the preparation, we used the Cu^{II}-Him complex $[Cu(Him)_4Cl]$-Cl as a starting building block, from which ligand recombination reactions with azides, the formation of the polymer structure and the growth of the single-crystals were successfully achieved under mild conditions. The X-ray analysis revealed that it has an im-bridged linear chain structure consisting of alternating dinuclear units with a symmetrical EO azide-bridged $[Cu(\mu_{1,1}\text{-}N_3)_2Cu]^{2+}$ core and mononuclear units. In spite of such a homometallic system, the magnetic susceptibility data showed ferrimagnetic-like behaviour. This could be explained by the combination of ferromagnetic coupling in the dinuclear core and antiferromagnetic coupling through the im bridges between the di- and the mononuclear units.

Experimental Section

Caution: Azides are potentially explosive. Only small amounts of this material should be prepared and handled with care.

$[Cu_3(Him)_4(im)_2(N_3)_4]_n$: An excess amount of sodium azide (300 mg, 4.6 mmol) in water (5 mL) was added to a saturated ethanol solution (50 mL) of $[Cu(Him)_4Cl]Cl$ (50 mg, 0.12 mmol), which changed the solution from blue to dark brown. Slow evaporation of the solvent yielded dark green crystals of $[Cu_3(Him)_4(im)_2(N_3)_4]_n$ with white crystals of sodium azide. These were washed with water to remove the latter crystals and the remainder was dried; yield 16 mg (52% based on Cu). $C_{18}H_{22}Cu_3N_{24}$ (765.17): calcd. C 28.25, H 2.90, N 43.93; found C 28.06, H 2.95, N 43.07.

X-ray Structural Analysis: The crystal data were collected with a Rigaku RAXIS-RAPID imaging plate diffractometer with graphite-monochromated Mo-K_α radiation (λ = 0.71075 Å). The structure was solved by direct methods (SHELX97) and expanded by using Fourier techniques. The non-hydrogen atoms were refined anisotropically. The hydrogen atoms were refined using the riding model. Structure refinements were performed using the full-matrix least-squares method on F^2. Calculations were performed using Crystal Structure software packages. Crystal data: $C_{18}H_{22}N_{24}Cu_3$, M = 765.17, triclinic, space group $P\bar{1}$, a = 7.6983(4) Å, b = 8.5720(7) Å, c = 22.6023(12) Å, α = 86.022(2), β = 82.7180(17), γ = 72.227(3), V = 1408.13(15), Z = 2, D_{calc} = 1.805 g/cm^3, μ(Mo-K_α) = 23.058 cm^{-1}, T = 90(2) K, 13580 reflections, 6359 unique, R_{int} = 0.044, R_1 [$I > 2.00\sigma(I)$] = 0.0659, wR_2 [$I > 2.00\sigma(I)$] = 0.1104, GOF = 0.999.

CCDC-783387 contains the supplementary crystallographic data for this paper. These data can be obtained free of charge from the Cambridge Crystallographic Data Centre via www.ccdc.cam.ac.uk/data_request/cif.

Magnetic Susceptibility: The measurements for temperature-dependent magnetic susceptibility and for a magnetization–magnetic field (M–H) curve were performed with a Quantum Design MPMS-XL5 SQUID magnetometer. For the former, a magnetic field of 1 T was applied, while for the latter, it was changed from 0 to +5 T.

Acknowledgments

This work was performed under the Cooperative Research Program of Network Joint Research Center for Materials and Devices (Research Institute for Electronic Science, Hokkaido University).

[1] C. Janiak, *Dalton Trans.* **2003**, 2781–2804.
[2] S. Kitagawa, R. Kitaura, S. Noro, *Angew. Chem. Int. Ed.* **2004**, *43*, 2334–2375.
[3] X. Zhao, B. Xiao, A. J. Fletcher, K. M. Thomas, D. Bradshaw, M. J. Rosseinsky, *Science* **2004**, *306*, 1012–1015.
[4] J. S. Seo, D. Whang, H. Lee, S. I. Jun, J. Oh, Y. J. Jeon, K. Kim, *Nature* **2000**, *404*, 982–986.
[5] C.-D. Wu, A. Hu, L. Zhang, W. Lin, *J. Am. Chem. Soc.* **2005**, *127*, 8940.
[6] M. D. Allendorf, C. A. Bauer, R. K. Bhakta, R. J. T. Houk, *Chem. Soc. Rev.* **2009**, *38*, 1330–1352.
[7] Y.-F. Zhag, X. Hu, Fu-C. Liu, X.-H. Bu, *Chem. Soc. Rev.* **2009**, *38*, 496–480.
[8] J. Ribas, A. Escuer, M. Monfort, R. Vicente, R. Cortés, L. Lezama, T. Rojo, *Coord. Chem. Rev.* **1999**, *193–195*, 1027–1068.
[9] X.-Y. Wang, Z.-M. Wang, S. Gao, *Chem. Commun.* **2008**, 281–294.
[10] A. Escuer, G. Aromi, *Eur. J. Inorg. Chem.* **2006**, 4721–4736.
[11] H. Ohtsu, Y. Shimazaki, A. Odani, O. Yamauchi, W. Mori, S. Itoh, S. Fukuzumi, *J. Am. Chem. Soc.* **2000**, *122*, 5733–5741.
[12] G. Kolks, S. J. Lippard, J. V. Waszczak, H. R. Lilienthal, *J. Am. Chem. Soc.* **1982**, *104*, 717–725.
[13] T. Glowiak, I. Wnek, *Acta Crystallogr., Sect. C* **1985**, *41*, 324–327.
[14] W. Wu, J. Xie, Y. Xuan, *J. Chem. Res.* **2008**, 344–346.
[15] J. Server-Carrió, E. Escrivà, J. V. Folgado, *Trans. Met. Chem.* **1996**, *21*, 541–545.
[16] D. L. McFadden, A. T. McPhail, C. D. Garner, F. E. Mabbs, *J. Chem. Soc., Dalton Trans.* **1975**, 263–268.
[17] P. Purkayastha, B. K. Sarma, A. N. Talukdar, *Indian J. Pure Appl. Phys.* **2003**, *41*, 350–353.
[18] T. Otieno, M. J. Hatfield, S. L. Asher, A. I. McMullin, B. O. Patrick, S. Parkin, *Synth. React. Inorg. Met. Org. Chem.* **2001**, *31*, 1587–1598.
[19] B. Wang, A. P. Côté, H. Furukawa, M. O'Keeffe, O. M. Yaghi, *Nature* **2008**, *453*, 207–211.
[20] N. Masciocchi, S. Bruni, E. Cariati, F. Cariati, S. Galli, A. Sironi, *Inorg. Chem.* **2001**, *40*, 5897–5905.
[21] J.-L. Lin, Y.-Q. Zheng, *Z. Kristallogr.* **2004**, *219*, 431–432.
[22] J.-P. Zhang, X.-M. Chen, *Chem. Commun.* **2006**, 1689–1699.
[23] X.-C. Huang, J.-P. Zhang, Y.-Y. Lin, X.-L. Yu, X.-M. Chen, *Chem. Commun.* **2004**, 1100–1101.
[24] T. C. Stamatatos, S. P. Perlepes, C. P. Raptopoulou, A. Terzis, C. S. Patrickios, A. J. Tasiopoulos, A. K. Boudalis, *Dalton Trans.* **2009**, 3354–3362.
[25] Sk. H. Rahaman, H. Chowdhury, D. Bose, G. Mostafa, H.-K. Fun, B. K. Ghosh, *Inorg. Chem. Commun.* **2005**, *8*, 1041–1044.
[26] G. A. V. Martins, P. J. Byrne, P. Allan, S. J. Teat, A. M. Z. Slawin, Y. Li, R. E. Morris, *Dalton Trans.* **2010**, *39*, 1785–1762.
[27] J.-R. Li, Q. Yu, E. C. Sañudo, Y. Tao, X.-H. Bu, *Chem. Commun.* **2007**, 2602–2604.
[28] W. Ouellette, A. V. Prosvirin, V. Chieffo, K. R. Dunbar, B. Hudson, J. Zubieta, *Inorg. Chem.* **2006**, *45*, 9346–9366.
[29] E. Ruiz, J. Cano, S. Alvarez, P. Alemany, *J. Am. Chem. Soc.* **1998**, *120*, 11122–11129.
[30] C. Adamo, V. Barone, A. Bencini, F. Totti, I. Ciofini, *Inorg. Chem.* **1999**, *38*, 1996–2004.
[31] M. A. Aebersold, B. Gillon, O. Plantevin, L. Pardi, O. Kahn, P. Bergerat, I. v. Seggern, F. Tuczek, L. Öhrström, A. Grand, E. Lelièvre-Berna, *J. Am. Chem. Soc.* **1998**, *120*, 5238–5245.
[32] L. Li, Z. Liu, S. S. Turner, D. Liao, Z. Jiang, S. Yan, *New J. Chem.* **2003**, *27*, 752–755.
[33] Q.-X. Jia, M.-L. Bonnet, E.-Q. Gao, V. Robert, *Eur. J. Inorg. Chem.* **2009**, 3008–3015.
[34] J. D. Woodward, R. V. Backov, K. A. Abboud, D. Dai, H.-J. Koo, M.-H. Whangbo, *Inorg. Chem.* **2005**, *44*, 638–648.
[35] S. Triki, C. J. Gómez-Garcia, E. Ruiz, J. Sala-Pala, *Inorg. Chem.* **2005**, *44*, 5501–5508.
[36] S. Koner, S. Saha, T. Mallah, K. Okamoto, *Inorg. Chem.* **2004**, *43*, 840–842.
[37] Y.-F. Wu, D.-R. Zhn, Y. Song, K. Shen, Z. Shen, X. Shen, Y. Xu, *Inorg. Chem. Commun.* **2009**, *12*, 959–963.
[38] A. Escuer, M. A. S. Goher, F. A. Mautner, R. Vicente, *Inorg. Chem.* **2000**, *39*, 2107–2112.
[39] S. Saha, S. Koner, J.-P. Tuchagues, A. K. Boudalis, K. Okamoto, S. Banerjee, D. Mal, *Inorg. Chem.* **2005**, *44*, 6379–6385.
[40] A. W. Addison, T. N. Rao, J. Reedijk, J. van Rijn, G. C. Verschoor, *J. Chem. Soc., Dalton Trans.* **1984**, 1349–1356.
[41] M. A. M. Abu-Youssef, A. Escuer, M. A. S. Goher, F. A. Mautner, G. J. Reiβ, R. Vicente, *Angew. Chem. Int. Ed.* **2000**, *39*, 1624–1626.
[42] A. Escuer, R. Vicente, M. S. El Fallah, M. A. S. Goher, F. A. Mautner, *Inorg. Chem.* **1998**, *37*, 4466–4469.
[43] M. A. M. Abu-Youssef, M. Drillon, A. Escuer, M. A. S. Goher, F. A. Mautner, R. Vicente, *Inorg. Chem.* **2000**, *39*, 5022–5027.
[44] A. Escuer, F. A. Mautner, M. A. S. Goher, M. A. M. Abu-Youssef, R. Vicente, *Chem. Commun.* **2005**, 605–607.
[45] Y.-M. Sun, C.-B. Liu, X. J. Lin, S.-W. Bi, *New J. Chem.* **2004**, *28*, 270–274.

Received: August 3, 2010
Published Online: November 24, 2010

